Atmos. Chem. Phys. Discuss., https://doi.org/10.5194/acp-2018-236
Manuscript under review for journal Atmos. Chem. Phys.
Discussion started: 7 March 2018

Atmospheric Chemistry and Physics
Open Access
Discussions

Observations of organic and inorganic chlorinated compounds and their contribution to chlorine radical concentrations in an urban environment in Northern Europe during the wintertime

Michael Priestley[1], Michael le Breton[1†], Thomas J. Bannan[1], Stephen D. Worrall[1^], Asan Bacak[1], Andrew R. D. Smedley[1*], Ernesto Reyes-Villegas[1], Archit Mehra[1], James Allan[1,2], Ann R. Webb[1], Dudley E. Shallcross[3], Hugh Coe[1], Carl J. Percival[1ǀ].

[1]Centre for Atmospheric Science, School of Earth and Environmental Sciences, University of Manchester, Manchester, M13 9PL, UK
[2]National Centre for Atmospheric Science, University of Manchester, Manchester, M13 9PL, UK
[3]School of Chemistry, The University of Bristol, Cantock's Close BS8 1TS, UK
[†]Now at Department of Chemistry and Molecular Biology, University of Gothenburg, 412 96 Göteborg, Sweden
^ Now at School of Materials, University of Manchester, Manchester, M13 9PL, UK
* Now at School of Mathematics, University of Manchester, Manchester, M13 9PL, UK
[ǀ]Now at Jet Propulsion Laboratory, 4800 Oak Grove Drive, Pasadena, CA 91109
Correspondence to: Carl Percival (carl.j.percival@jpl.nasa.gov)

Abstract. A number of inorganic (nitryl chloride, $ClNO_2$; chlorine, Cl_2; and hypochlorous acid, HOCl) and chlorinated, oxygenated volatile organic compounds (ClOVOCs) have been measured in Manchester, UK during October and November 2014 using time of flight chemical ionisation mass spectrometry (ToF-CIMS) with the I^- reagent ion. ClOVOCs appear to be mostly photochemical in origin although direct emission from vehicles is also suggested. Peak concentrations of $ClNO_2$, Cl_2 and HOCl reach 506, 16 and 9 ppt respectively. The concentrations of $ClNO_2$ are comparable to measurements made in London, but measurements of ClOVOCs, Cl_2 and HOCl by this method are the first reported in the UK. Maximum HOCl and Cl_2 concentrations are found during the day and $ClNO_2$ concentrations remain elevated into the afternoon if photolysis rates are low. Cl_2 exhibits a strong dependency on shortwave radiation further adding to the growing body of evidence that it is a product of secondary chemistry, however night time emission is also observed. The contribution of $ClNO_2$, Cl_2 and ClOVOCs to the chlorine radical budget suggests that Cl_2 can be a greater source of Cl than $ClNO_2$, contributing 57% of the Cl radicals produced on a high radiant flux day. In contrast, on a low radiant flux day, this drops to 17% as both Cl_2 production and loss pathways are inhibited by reduced photolysis rates. This results in $ClNO_2$ making up the dominant fraction (68%) on low radiant flux days as its concentrations are still high. As most ClOVOCs appear to be formed photochemically, they exhibit a similar dependence on photolysis, contributing between 15% - 24% of the Cl radical budget observed here.

1. Introduction

Oxidation controls the fate of many atmospheric trace gases. For example, increasing the oxidation state of a given species may increase its deposition velocity (Nguyen et al. 2015) or solubility (Carlton et al. 2006) and reduce its volatility (Carlton et al. 2006), all of which act to reduce the atmospheric lifetime of that species and can lead to the formation of secondary material such as secondary organic aerosol (SOA) or ozone (O_3). As the identity of the chemical species change with oxidation, intrinsic and diverse properties of the chemical species are altered; influencing their toxicity (Borduas et al. 2015) and their impact on the environment e.g. cloud particle nucleating efficiency (Ma et al. 2013) or global warming potential (Boucher et al. 2009).

The hydroxyl radical (OH) is considered the most important daytime atmospheric oxidant due to its ubiquity and high reactivity with an average tropospheric concentration of 10^6 molecules cm^{-3} (Heal et al. 1995). However, rate coefficients for the reaction of the chlorine radical (Cl) can be two orders of magnitude larger than those for OH (Spicer et al. 1998) indicating that lower Cl concentrations of $1x10^4$ atoms cm^{-3} that are estimated to exist in urban areas (e.g. Bannan et al., 2015), can be just as significant in their contribution to oxidation.

Cl initiated oxidation of volatile organic compounds (VOCs) forms chlorinated analogues of the OH initiated oxidation products, via addition (1) or hydrogen abstraction (2) forming HCl that may react with OH to regenerate Cl. Subsequent peroxy-radicals formed through Cl oxidation can take part in the HO_x cycle and contribute to the enhanced formation of O_3 and SOA (Wang & Ruiz 2017).

$$R + X \xrightarrow{O_2} R(X)OO^{\cdot} \quad (1)$$

$$RH + X \xrightarrow{O_2} ROO^{\cdot} + HX \quad (2)$$

where X is OH or Cl.

Nitryl chloride ($ClNO_2$) is a major reservoir of Cl that is produced by aqueous reactions between particulate chloride (Cl^-) and nitrogen pentoxide (N_2O_5) (4, 5). Gaseous $ClNO_2$ is produced throughout the night and is typically photolysed at dawn before $^{\cdot}OH$ concentrations reach their peak (6). This early morning release of Cl induces oxidation earlier in the day and has been shown to increase maximum 8 hour mean O_3 concentrations by up to 7 ppb under moderately elevated NO_x levels (Sarwar et al. 2014). Typical $ClNO_2$ concentrations measured in urban regions range from 10s of ppt to 1000s of ppt. Mielke et al. (2013) measured a maximum of 3.6 ppb (0.04Hz) during summer time in L.A. with maximum sunrise concentrations of 800 ppt. Bannan et al. (2015) measured a maximum concentration of 724 ppt (1Hz) at an urban background site in London during summer. They state that in some instances, $ClNO_2$ concentrations increase after sunrise and attribute this to the influx of air masses with higher $ClNO_2$ concentrations by either advection or from the collapse of the residual mixing layer. In urban environments where NO_x emission and subsequent N_2O_5 production is likely, Cl^- may be the limiting reagent in the formation of $ClNO_2$ if excess NO does not reduce NO_3 (3) before N_2O_5 is produced (e.g. Bannan et al., 2015). Whilst distance from a marine source of Cl^- may explain low, inland concentrations (Faxon et al. 2015), long range transport of marine air can elevate inland $ClNO_2$ concentrations (Phillips et al. 2012) and long range transport of polluted plumes to a marine location can also elevate $ClNO_2$ concentrations (e.g. Bannan et al. 2017).

$$NO_3 + NO \longrightarrow 2NO_2 \quad (3)$$

$$NO_3 + NO_2 \longrightarrow N_2O_{5(g)} \longrightarrow N_2O_{5(aq)} \quad (4)$$

$$Cl^- + N_2O_5 \longrightarrow ClNO_2 + NO_3^- \quad (5)$$

$$ClNO_{2(aq)} \longrightarrow ClNO_{2(g)} \xrightarrow{J_{ClNO_2}} Cl + NO_2 \quad (6)$$

Anthropogenic emission of molecular chlorine is identified as another inland source of Cl^- in the U.S. (e.g. Thornton et al. 2010; Riedel et al. 2012) and in China (e.g. Wang et al. 2017, Liu et al. 2017) where some of the highest concentrations 3.0 - 4.7 ppb have been recorded. As well as industrial processes, the suspension of road salt used to melt ice on roads during the winter has been suggested as a large source of anthropogenic Cl^- (Mielke et al. 2016). This winter time only source, combined with reduced nitrate radical photolysis, is expected to yield greater $ClNO_2$ concentrations at this time of the year (Mielke et al. 2016).

The photolysis of molecular chlorine (Cl_2) is another potential source of Cl. Numerous heterogeneous formation mechanisms leading to Cl_2 from Cl^- containing particles are known. These include the reaction of Cl^- and OH (Vogt et al. 1996), which may originate from the photolysis of $O_{3(aq)}$ (Oum 1998) or reactive uptake of $ClNO_2$ (Leu et al. 1995), $ClONO_2$ (Deiber et al. 2004) or HOCl (Eigen & Kustin 1962) to acidic Cl^- containing particles. Thornton et al. (2010) also suggest that inorganic Cl resevoirs such as HOCl and $ClONO_2$ may also enhance the Cl concentration, potentially accounting for the short fall in the global burden (8-22 Tg yr^{-1} source from $ClNO_2$ and 25-35 Tg yr^{-1} as calculated from methane isotopes). These may be directly through photolysis or indirectly through heterogenous reactions with Cl^- on acidic aerosol.

Globally, Cl_2 concentrations are highly variable. In the marine atmosphere, concentrations up to 35 ppt have been recorded (Lawler et al. 2011) whereas at urban costal sites in the US, concentrations on the order of 100s ppt have been measured (Keene et al. 1993, Spicer et al. 1998). Sampling urban outflow, Riedel et al. (2012) measure a maximum of 200 ppt Cl_2 from plumes and mean concentrations of 10 ppt on a ship in the LA basin. Maximum mixing ratios of up to 65 ppt have also been observed in the continental US (Mielke et al. 2011).

More interestingly, these studies (Keene et al. 1993; Spicer et al. 1998; Lawler et al. 2011; Mielke et al. 2011), report maximum Cl_2 concentrations at night and minima during the day. However, there is a growing body of evidence suggesting day time Cl_2 may also be observed. Although primary emission may be one source of daytime Cl_2 (Mielke et al. 2011), others demonstrate the diurnal characteristics of the Cl_2 time series has a broader signal suggestive of continuous processes rather than intermittent signals typically associated with sampling emission sources under turbulent conditions.

In a clean marine environment Liao et al. (2014) observe maximum Cl_2 concentrations of 400 ppt attributed to emission from a local snow pack source. A maxima was measured during the morning and evening with a local minimum during mid-day caused by photolysis. They also describe negligible night time concentrations, with significant loss attributed to deposition. Faxon et al. (2015) measured Cl_2 with a ToF-CIMS recording a maximum during the afternoon of 4.8 ppt (0.0016 Hz) and suggest a local precursor primary source of Cl_2, potentially soil emission, with further heterogeneous chemistry producing Cl_2. At a rural site in north China, Liu et al. (2017) measured mean concentrations of Cl_2 of 100 ppt and a maximum of 450 ppt, peaking during the day; they also report 480 ppt observed in an urban environment in the US during summer. They attribute power generation facilities burning coal as the source.

Another potential source of Cl to the atmosphere is the photolysis of chlorinated organic compounds (ClVOCs, chlorocarbons, organochlorides) that are emitted from both natural (biomass burning, oceanic and biogenic emission) (e.g. Yokouchi et al. 2000) and anthropogenic sources (e.g. Butler 2000). Whilst many ClVOCs are

Atmos. Chem. Phys. Discuss., https://doi.org/10.5194/acp-2018-236
Manuscript under review for journal Atmos. Chem. Phys.
Discussion started: 7 March 2018

Atmospheric Chemistry and Physics Discussions

only considered chemically important in the stratosphere, those that are photochemically labile in the troposphere e.g. methyl hypochlorite (CH_3OCl) whose absorption cross section is non-negligible at wavelengths as long as 460 nm (Crowley et al. 1994), can act as a source of Cl and take part in oxidative chemistry.

Photolysis of ClVOCs have been postulated to contribute 0.1 - 0.5 $\times 10^3$ atoms cm^{-3} globally to the Cl budget of the boundary layer (Hossaini et al. 2016), although on much smaller spatial and temporal scales, the variance in this estimate is likely to be large. Very little data exist~~s~~ on the concentrations, sources and spatial extent of oxygenated ClVOCs (ClOVOCs) and their contribution to the Cl budget.

The ToF-CIMS is a highly selective and sensitive instrument with a high mass accuracy and resolution (m/dm ~4000) that is capable of detecting a suite of chlorinated compounds including HOCl, $ClONO_2$ and organic chlorines (Le Breton et al. 2018), as well as other oxygenated chlorine species and chloroamines (Wong et al. 2017). Here we use the ToF-CIMS with the I^- reagent ion to characterise the sources of chlorine and estimate their contribution to Cl concentrations in winter time Manchester, UK.

2. Methodology / experimental

Full experimental details and description of meteorological and air quality measurements can be found in Priestley et al. (2018). A time of flight chemical ionisation mass spectrometer (ToF-CIMS) (Lee et al. 2014) using iodide reagent ions was used to sample ambient air between 2014-10-29 and 2014-11-11 at the University of Manchester's south campus, approximately 1.5 km south of Manchester City Centre, UK (N53.467, W2.232) and 55 km east of the Irish Sea. Sample loss to the 1m long ¾" PFA inlet was minimised by using a fast inlet pump inducing a flow rate of 15 standard litres per minute (slm) which was subsampled by the ToF-CIMS. Backgrounds were taken every 6 hours for 20 minutes by overflowing dry N_2. Formic acid was calibrated throughout the campaign and post campaign. A number of chlorinated species were calibrated post campaign using a variety of different methods and relative calibration factors were applied based on measured instrument sensitivity to formic acid as has been performed previously (e.g. le Breton et al. 2014; le Breton et al. 2017; Bannan et al. 2015). A summary of calibration procedures and species calibrated are described below. All data from between 16:30 on the 5th of November to midnight on the 7th of November has been removed to prevent the interference of a large scale anthropogenic biomass burning event (Guy Fawkes Night) on these analyses.

2.1. Calibrations

We calibrate a number of species by overflowing the inlet with various known concentrations of gas mixtures (Le Breton et al. 2012), including molecular chlorine (Cl_2, 99.5% purity, Aldrich), formic acid (98/100%, Fisher) and acetic acid (glacial, Fisher) by making known mixtures (in N_2) and flowing 0-20 standard cubic centimetres per minute (sccm) into a 3 slm N_2 dilution flow that is subsampled. As all chlorinated VOCs we observe are oxygenated, we assume the same sensitivity found for acetic acid for the rest of the organic chlorine species detected. The instrument sensitivity to dichloromethane (DCM, VWR) and chloroform ($CHCl_3$, 99.8%, Aldrich) were also quantified, but these species were not detected during ambient sampling. Methyl chloride (CH_3Cl) and chlorovaleric acid were also detected in the laboratory but not quantified.

$ClNO_2$ was calibrated by the method described by Kercher et al. (2009) with N_2O_5 synthesised following the methodology described by Le Breton et al. (2014). Excess O_3 is generated by flowing 200 sccm O_2 (BOC) through an ozone generator (BMT, 802N) and into a 5 litre glass volume containing NO_2 (sigma, >99.5%). The outflow from this reaction vessel is cooled in a cold trap held at -78°C (195 K) by a dry ice/glycerol mixture where N_2O_5 is condensed and frozen. The trap is allowed to reach room temperature and the flow is reversed where it is then condensed in a second trap held at 195 K. This process is repeated several times to purify the mixture. The system is first purged by flowing O_3 for ten minutes before use. To ascertain the N_2O_5 concentration on the line, the flow is diverted through heated line to decompose the N_2O_5 and into to a Thermo Scientific 42i NO_x analyser where it is detected as NO_2. It is known that the Thermo Scientific 42i NO_x analyser suffers from interferences from NO_y species, indicating that this method could cause an underestimation of the $ClNO_2$ concentrations reported here. Based on previous studies (e.g. Le Breton et al. 2014; Bannan et al. 2017) where comparisons with a broad beam cavity enhancement absorption spectrometer (BBCEAS) have been made, good agreement has been found between co-located N_2O_5 measurements. We feel that this calibration method works well, likely in part due to the high purity of N_2O_5 synthesised and the possible interference of NO_y on the NO_x analyser during this calibration is considered negligible. The N_2O_5 is passed over a salt slurry where excess chloride may react to produce $ClNO_2$. The drop in N_2O_5 signal is equated to the rise in $ClNO_2$ as the stoichiometry of the reaction is 1:1. The conversion efficiency of N_2O_5 to $ClNO_2$ over wet NaCl is known to vary by between 60-100% (Hoffman et al. 2003; Roberts et al. 2008). Here we follow the methodology of Osthoff et al. (2008) and Kercher et al. (2009) that ensure conversion is 100% efficient and so we assume 100% yield in this study.

We utilise a second method to verify our first $ClNO_2$ calibration by cross calibration with a turbulent flow tube chemical ionisation mass spectrometer (TF-CIMS) (Leather et al. 2012). We flow a known concentration of 0-20 sccm Cl_2 (99.5% purity Cl_2 cylinder, Aldrich) from a diluted (in N_2) gas mix into an excess constant flow of 20 sccm NO_2 (99.5% purity NO_2 cylinder, Aldrich) from a diluted (in N_2) gas mix, to which the TF-CIMS has been calibrated. This flow is carried in 52 slm N_2 that is purified by flowing through two heated molecular sieve traps. This flow is subsampled by the ToF-CIMS where the $I.ClNO_2^-$ adduct is measured. The TF-CIMS is able to quantify the concentration of $ClNO_2$ generated in the flow tube as the equivalent drop in NO_2^- signal. This indirect measurement of $ClNO_2$ is similar in its methodology to $ClNO_2$ calibration by quantifying the loss of N_2O_5 reacted with Cl^- (e.g. Kercher et al. 2009). We assume the same sensitivity for $ClONO_2$ as $ClNO_2$. We do not detect an increase in $I.Cl_2$ signal from this calibration and so rule out the formation of Cl_2 from inorganic species in our inlet due to unknown chemistry occurring in the IMR. The TF-CIMS method gives a calibration factor 58% greater than that of the N_2O_5 synthesis method therefore this is taken as our measurement uncertainty.

We calibrate HOCl using the methodology described by Foster et al. (1999). 100 sccm N_2 is flowed through a fritted bubbler filled with NaOCl solution (min 8% chlorine, Fisher) that meets a dry 1.5 slm N_2 flow, with the remaining flow made up of humidified ambient air, generating the HOCl and Cl_2 signal measured on the ToF-CIMS. The flow from the bubbler is diverted through a condensed HCl (sigma) scrubber (condensed HCl on the wall of 20cm PFA tubing) where HOCl is titrated to form Cl_2. The increase in Cl_2 concentration when the flow is sent through the scrubber is equal to the loss of HOCl signal and as the calibration factor for Cl_2 is known, the relative calibration factor for HOCl to Cl_2 is found.

Atmos. Chem. Phys. Discuss., https://doi.org/10.5194/acp-2018-236
Manuscript under review for journal Atmos. Chem. Phys.
Discussion started: 7 March 2018

2.2. Cl radical budget calculations

Within this system, we designate $ClONO_2$, $ClNO_2$, HOCl and organic chlorine as sources of Cl. As HCl measurements were not made, it is not possible to quantify the contribution of Cl from the reaction of HCl + OH. Loss processes of Cl are Cl + O_3 and Cl + CH_4 (7). Photolysis rates for the Cl sources are taken from the NCAR Tropospheric Ultraviolet and Visible TUV radiation model (Mandronich 1987) assuming 100% quantum yield at our latitude and longitude with column overhead O_3 measured by Brewer spectrophotometer #172 (Smedley et al. 2012) and assuming zero optical depth. To account for the effective optical depth of the atmosphere including clouds and other optical components, we scale our idealised photolysis rate coefficient (*J*) by the observed transmittance values in the UV-A waveband (325 to 400 nm). These transmittance values are calculated from UV spectral scans of global irradiance, measured at half-hourly intervals by Brewer spectrophotometer and provided as an output of the shicRIVM analysis routine (Slaper et al. 1995). The Cl rate coefficient for the reaction with O_3 is k_{Cl+O3} = 1.20 x 10^{-11} cm^3 $molecule^{-1}$ s^{-1} (Atkinson et al. 2007) and CH_4 is k_{Cl+CH4} = 1.03 x 10^{-13} cm^3 $molecule^{-1}$ s^{-1} (Atkinson et al. 2006).

$$[Cl]_{SS} = \frac{2J_{Cl_2}[Cl_2]+J_{ClNO_2}[ClNO_2]+J_{HOCl}[HOCl]+J_{ClONO_2}[ClONO_2]}{k_{\mathrm{O_3+Cl}}[\mathrm{O_3}]+k_{\mathrm{CH_4+Cl}}[\mathrm{CH_4}]} \tag{7}$$

As methane and VOCs were not measured, an average CH_4 concentration taken from ECMWF Copernicus atmosphere monitoring service (CAMS) was used. The photosensitivity of the ClOVOCs to wavelengths longer than 280 nm dictates their ability to contribute to the Cl budget in the troposphere. As many of the identified species here do not have known photolysis rates, we approximate the photolysis of methyl hypochlorite J_{CH3OCl} for all ClOVOCs as it is the only available photolysis rate for an oxygenated organic compound containing a chlorine atom provided by the TUV model. The same quantum yield and actinic flux assumptions are made.

2.3. Identification by mass defect

Whilst looking for signal in the spectra with high mass defects, indicative of compounds containing multiple Cl atoms, various signals with the I_2 cluster as a reagent ion were detected. ToF-CIMS reagent ions such as HNO_3/NO_3 and H_2SO_4/HSO_4 are known to form dimer, trimer and tetramer clusters which serve as additional ionisers (e.g. Sipilä et al. 2015; Simon et al. 2016). It is also known that ionisation with I^- forms I_2^- and I_3^- clusters, which are often used as mass calibrants. Many of the I_2 adducts measured here are formed with fragments such as O and CN that are likely a consequence of IMR chemistry, however in this instance, we find $I_2.NO_2$ a useful measurement of NO_2/NO_y.

Fig 1. demonstrates the strong agreement (R^2 = 0.93) between the $I_2.NO_2^-$ adduct as measured on the ToF-CIMS and the NO_2 measurement of a Thermo Scientific 42i NO_x analyser at the Whitworth Observatory. Chemiluminescence techniques used for the detection of NO_x species, like that employed by the Thermo Scientific 42i NO_x analyser, are known to overestimate NO_2 concentrations through the additional contribution of NO_y (e.g. Reed et al. 2016). Here we observe a non-linear increase in signal from the ToF-CIMS, indicating its susceptibility to interference at higher concentrations is greater than that of the NO_x analyser. The cause is unclear but is likely fragmentation of NO_y in the IMR. This diagnosis is consistent with the largest discrepancy between the measurements being found during bonfire night (5^{th} Nov) which is a large source of organic nitrates (Reyes-Villegas et al. 2017). When the $(NOy-NO_2):NO_2$ ratio is low, more typical in cleaner environments, the $I_2.NO_2^-$ adduct may be useful as a measurement for NO_2.

3. Results

Concentrations of all chlorinated species are higher at the beginning of the measurement campaign when air masses originating from continental Europe were sampled (Reyes-Villegas et al. 2017). Toward the end of the measurement campaign $ClONO_2$ and ClOVOCs concentrations were low which is consistent with the pollution during this period having a high fraction of primary components (Reyes-Villegas et al. 2017), see Fig 2.

3.1. Inorganic chlorine

We detect a range of inorganic chlorine species and fragments including $I.Cl^-$, $I.ClO^-$, $I.HOCl^-$, $I.Cl_2^-$, $I.ClNO_2^-$ and $I.ClONO_2^-$ however we do not detect $I.ClO_2^-$, $I.Cl_2O^-$, $I.Cl_2O_2^-$, $I.ClNO^-$ or $I.HCl^-$. Laboratory studies have shown that the ToF-CIMS is sensitive to detection of $I.HCl^-$, however under this configuration, the $I.HCl^-$ adduct was not observed. N_2O_5 was measured during the campaign however a strong daytime interference at 235 m/z identified as $C_2H_4O_5$ (tentatively assigned as hydroperoxy(hydroxy)acetic acid, hydroxy acetic hydroperoxide, HAHP), means this signal cannot be utilised during the day. The statistics of the concentrations reported below do not take into account the limits of detection (LOD) and so for some of the measurements, values may be reported below the LOD.

3.1.1. $ClNO_2$ and $ClONO_2$

$ClNO_2$ (m/z 208) was detected every night of the campaign with a LOD (3x standard deviation of the background) of 3.8 ppt. The night time N_2O_5 signal anti-correlates with NO as expected, whereas the $ClNO_2$ signal shows no correlation with NO which is also expected if $ClNO_2$ is not being produced in the inlet. The 1Hz mean night time concentration of $ClNO_2$ was 58 ppt (not accounting for the LOD) and a maximum of 506 ppt (not accounting for the LOD) was measured as a large spike on the evening of the 30th Oct. These concentrations are comparable to other urban U.K. measured values although the maximum concentration reported here is 30% lower than that measured in London (Bannan et al. 2015) but is consistent with high concentrations expected during the winter as discussed in the introduction.

The diurnal profile of $ClNO_2$ increases through the evening to a local morning maximum with rapid loss after sunrise. Although we observe a rapid build-up after sunset (ca. 16:30) and loss after sunrise (ca. 07:30), the maximum concentration measured within a given 24 hour period typically peaks at around 22:00 and halves by 03:00 where it is maintained. The reasons for the early onset in peak concentration and loss throughout the night is unclear although on 1st Nov, a sharp decrease in $ClNO_2$ is a consequence of a change in wind direction, indicating the source of $ClNO_2$ is directional. A minimum concentration of <LOD is reached by 15:00 indicating concentrations can persists for much of the day. On 7th Nov $ClNO_2$ concentrations grow throughout the morning even after photolysis begins until 11:00. Correlated high wind speeds suggest long range transport and downward mixing is a likely cause for this daytime increase.

Typically, elevated concentrations of $ClNO_2$ are measured when the wind direction is easterly and wind speeds are low (2-4 ms^{-1}) and also during periods of southerly winds between 3-9 ms^{-1}. The potential sources of Cl^- precursor from these directions are industrial sites, including waste water treatment facilities (8.5 km east and 7.0 km south) that may use salt water as part of the chemical disinfection process (Ghernaout & Ghernaout 2010). Another source of $ClNO_2$ precursor is found from the south west at wind speeds of 9 ms^{-1} indicating a more distant source which is also likely to be industrial/marine. The correlation between $ClNO_2$ and Cl_2 is poor at most times apart from the night of the 30th where a strong linear relationship is observed. This is consistent with polluted continental air masses advecting a variety of trace gases. Throughout the measurement campaign the relationship between $ClNO_2$ and Cl_2 is poor and so it is unlikely they share the same source. Maximum $ClONO_2$ concentrations reach 20.3 ppt. The average concentration is 2.0 ppt (not accounting for the LOD) and LOD of 0.9 ppt. The behaviours of $ClONO_2$ and $ClNO_2$ are extremely similar (R^2=0.97).

3.1.2. HOCl

HOCl concentrations average 2.18 ppt (not accounting for the LOD) and reach a daytime maximum of 9.28 ppt with an LOD of 3.8 ppt. Concentrations peak in the early afternoon similarly to Cl_2 but remain elevated for longer, dropping after sunset. The diurnal profile is similar to that for O_3 with a maximum during the day and minima during morning and evening rush hours when NO_x is emitted locally. The strong correlation with O_3 (R^2 = 0.67) is expected as the route to formation of HOCl is the oxidation of Cl with O_3 to form ClO and then oxidation by HO_2 to form HOCl. Non negligible night time concentrations of a maximum 8.1 ppt are only measured when concentrations of other inorganic Cl containing species are high. The HOCl signal is artificially elevated after the night of the 5th due to a persistent interference from a large scale biomass burning event that cannot be deconvolved from the dataset (Guy Fawkes Night, Priestley et al., 2018). For this reason HOCl data after this date are discounted from the analysis.

3.1.3. ClO

We detect the $I.ClO^-$ adduct at *m/z* 178 which strongly correlates with $I.ClNO_2^-$, $I.ClONO_2^-$ and $I.Cl^-$ signals, all of which show night time maxima. This is inconsistent with the ClO photochemical production pathway of Cl + O_3 suggesting its maximum concentration should be measured during the day as was observed for HOCl. It is not possible to confirm if the $I.ClO^-$ is a fragment of a larger ClO containing molecule, however, as the fragmentation of multiple larger molecules are detected as a single adduct e.g. the $I.Cl^-$ cluster is a known fragment from $ClNO_2$ and HOCl, it is reasonable to suspect $I.ClO^-$ may be a fragment as well.

3.1.4. Cl_2

We observe concentrations of Cl_2 during the day ranging from 0 – 16.6 ppt with a mean value of 2.3 ppt (not accounting for the LOD) and night time concentrations of 0 – 4.7 ppt with mean concentrations of 0.4 ppt (not accounting for the LOD), see Fig 2. The LOD is 0.5 ppt. These concentrations are of the same order of magnitude as measured at an urban site in the U.S. but up to 2 orders of magnitude smaller than at U.S urban costal sites (Keene et al. 1993, Spicer et al. 1998) and a megacity impacted rural site in north China (Liu et al. 2017). Although the maximum measured value here is an order of magnitude greater than that measured in Houston (Faxon et al. 2015), the photolysis rate of Cl_2 here is two orders of magnitude smaller compared with Houston at that time.

The diurnal profile of Cl_2 exhibits a maximum at midday and a minimum at night (early morning) consistent with other studies (Liao et al. 2014; Faxon et al. 2015; Liu et al. 2017). The days with the greatest concentration are those where direct shortwave radiation is at its highest. On the 5th of November, the incidence of direct shortwave radiation is unhindered throughout the day and a similarly uniform profile for Cl_2 is also observed. On the 1st of November, Cl_2 concentrations increase unhindered as direct radiation increases but when cloud cover reduces radiation transmission efficiency, a corresponding drop in Cl_2 is also observed (Fig 3). Equally when global radiation is low throughout the day e.g. 7th November, we observe very low concentrations of Cl_2.

There is the potential that the Cl_2 signal detected is an instrumental artefact generated either by chemistry in the IMR or from displacement reactions or degassing on the inlet walls. We believe none of these to be the case. First, the correlation between the signal used for labile chlorine in the IMR ^{35}Cl (*m/z 35*) is high with $ClNO_2$ (R^2=0.98) yet is non-existent with Cl_2 (R^2=0.01) indicating Cl_2 concentration is independent of ^{35}Cl concentrations. Second, there is no correlation between HNO_3 and Cl_2 (R^2=0.07) which suggests that acid displacement reactions are not occurring on the inlet walls. Third, there is no correlation between temperature and Cl_2 (R^2=0.08) indicating that localised ambient inlet heating is also not a contributing factor to increased Cl_2 concentrations. Fourth, we observe a similar direct radiation dependency for other photochemical species as we observe for Cl_2. For example, the temporal behaviour of $C_2H_4O_5$ (potentially hydroxy acetonehydroxy peroxide, HAHP, a photochemical marker and known product of aqueous ozone chemistry (Leitzke et al. 2001)) exhibits a similar diurnal profile and radiation dependency (Fig 3). Also, the production of O_3 increases and decreases with direct solar radiation at the same times we observe the enhancements in concentrations of Cl_2 and $C_2H_4O_5$ (Fig 3). The changes in O_3 production are observed when NO concentrations are near zero indicating O_3 production is VOC limited. Finally, other large organic molecules e.g. $C_{10}H_{14}O_4$ do not exhibit this strong coupling with direct solar radiation. This evidence suggests a local photolytic daytime mechanism is responsible for the increase in daytime concentrations as has previously been suggested (e.g. Finley & Saltzman 2006).

Although peak concentrations of Cl_2 are observed in the daytime, high levels of Cl_2 are also observed during the night. At the beginning of the measurement period, which has previously been characterised using an aerosol mass spectrometer (AMS) as a period of high secondary activity (Reyes-Villegas et al. 2017), there are persistent, non-zero concentrations of Cl_2 ($\leq$ 4 ppt) after sunset. On the 4th November, after the period of high secondary activity, intermittent elevations in night time Cl_2 concentrations, when the wind is northerly, suggest a local emission source, with concentrations reaching a maximum of 4.6 ppt. Two more distinct night time sources, ranging from the south west through to the east of the measurement site indicate a likely origin of industrial areas, some of which contain chemical production and water treatment facilities.

3.2. Organic chlorine

We detected seven C_2-C_6 ClOVOCs of the forms $C_nH_{2n+1}O_1Cl$, $C_nH_{2n+1}O_2Cl$, $C_nH_{2n+1}O_3Cl$, $C_nH_{2n-1}O_2Cl$, $C_nH_{2n-1}O_3Cl$, $C_nH_{2n-3}O_2Cl$ (Fig 4) of which only $C_2H_3O_2Cl$ has been reported before (Le Breton et al. 2018). We find no evidence for the detection of small chlorohydrocarbons e.g. poly-chloromethanes, such as methyl chloride, dimethyl chloride and chloroform, or poly-chloroethanes such as those described by Huang et al. (2014), but our laboratory calibrations show that the iodide reagent ion is sensitive to CH_3Cl, CH_2Cl_2 and $CHCl_3$ albeit with a high LOD. We find no discernable evidence for the detection of 4-chlorocrotonaldehyde, the Cl oxidation product of 1,3-butadiene and unique marker of chlorine chemistry (Wang & Finlayson-Pitts 2001) due to interferences from other CHO compounds.

The maximum hourly averaged total ClOVOCs concentration is 140 ppt at midday and at a minimum of 80 ppt at 07:00 when NO_x concentrations are highest at ~30 ppb. Concentrations of $C_2H_3O_2Cl$ (tentatively identified as chloroacetic acid) and $C_6H_{13}OCl$ (tentatively identified as chloro-hexanol) are the highest of any ClOVOCs, accounting for between 20% and 30% respectively of total ClOVOCs concentrations measured. All

Atmos. Chem. Phys. Discuss., https://doi.org/10.5194/acp-2018-236
Manuscript under review for journal Atmos. Chem. Phys.
Discussion started: 7 March 2018

concentrations rise towards midday with $C_3H_7O_2Cl$ and $C_2H_3O_2Cl$ rising the most by a factor of 1.8 and returning to nominal levels by the early evening (red in Fig 4). $C_3H_7O_2Cl$ and $C_2H_3O_2Cl$ correlate well with Cl_2 (R^2 0.76, 0.62 respectively) which is consistent with a photochemical formation mechanism identifying these species as secondary products, potentially, chloro-propanediol and chloro-acetic acid.

Whilst the diurnal profiles of $C_6H_{13}OCl$, $C_3H_5O_3Cl$ and $C_5H_7O_2Cl$ (blue in Fig 4) are similar to those of $C_3H_7O_2Cl$ and $C_2H_3O_2Cl$, they do not enhance as much as those photochemical species or return to nominal levels after the solar maximum, instead they increase again during the night, with $C_3H_5O_3Cl$ reaching a maximum concentration of 8 ppt at 20:00. This trend suggests concentration changes could be a function of boundary layer height.

$C_3H_5O_2Cl$ and $C_4H_7O_2Cl$ (yellow in Fig 4) are the only ClVOCs that show a positive correlation with NO_x (R^2=0.47, R^2=0.26) and negative correlation with O_3 (R^2=-0.58, R^2=-0.34). Their correlation is stronger with NO_2 (R^2=0.57, R^2=0.34), a product of traffic emission. This suggests that at least some of the time, they accumulate at low wind speeds, indicating their origins as local, primary emissions, or as thermal degradation products that have a traffic source e.g. polychlorinated dibenzo-*p*-dioxins/dibenzofurans (PCDD/F) and their oxidation products (Fuentes et al. 2007; Heeb et al. 2013). The diurnal profile shows maxima during mid-day consistent with other photochemical species which is expected of secondary formation. It is possible that these compounds are isobaric or isomeric with other compounds that interfere with the perceived signals recorded here.

4. Discussion

4.1. Effect of global radiation transmission efficiency on Cl radical production

Three days are selected based on their different solar short wave transmission efficiencies to quantify the variation in Cl_2 formation and photolysis and so the influence of Cl_2 on producing Cl. The average transmission of global radiation on the 5th of November was high, 84 ± 14% (1σ), whereas on the 7th of November it was very low 21 ± 14%, sometimes dropping below 10% in the middle of the day. The 1st of November serves as a middle case where the transmission efficiency in the morning was high, 88 ± 11% but in the afternoon was highly variable and dropped to 55% ± 20% see Fig 5. These three days provide good case studies to investigate the effect of global radiation on molecular chlorine concentrations and therefore the production of Cl.

The reduced transmission efficiency inhibits Cl_2 formation thereby reducing the contribution of Cl_2 to Cl production. The lower transmission efficiency also reduces the photolysis of Cl_2 and so reduces the production of Cl even further. Fig 6. shows the divergence between the ideal J_{Cl2} without transmission efficiency correction (a) and the J_{Cl2} value scaled by transmission efficiency (b) and subsequent Cl formation. Cl production rates are similar until 11am when the scaled production then becomes on average 47% lower. This is most prominent at 13:00 when the difference between ideal and scaled production is 8.4×10^4 Cl radicals cm^{-3} s^{-1}.

4.2. Contribution of inorganic chlorine to Cl radical production

The contribution of HOCl and $ClONO_2$ to Cl formation is negligible due to low photolysis rates and low concentrations whereas the contribution from Cl_2, $ClNO_2$ and ClOVOCs is much greater (Fig 7). During the morning of the 1th and 5th Nov, $ClNO_2$ is the dominant source of Cl contributing 95% of total Cl concentration, a maximum of 1.3 x 10^3 Cl radicals cm^{-3} to the steady state concentration which is approximately a factor of ten lower than the estimated maximum concentration of 9.5 × 10^3 Cl radicals cm^3 produced by $ClNO_2$ photolysis in London during the summer (Bannan et al. 2015) and a factor of 65 lower than the maximum concentration of 85.0 × 10^3 Cl radicals cm^{-3} calculated from measurements of $ClNO_2$ in Houston (Faxon et al. 2015). In both instances this is due to a combination of lower J_{ClNO2} and lower $ClNO_2$ concentrations.

As the day progresses, concentrations of Cl_2 increase and it becomes the dominant and more sustained source of Cl contributing 95% of Cl (16.8 x 10^3 Cl radicals cm^{-3}) by the early afternoon, which is approximately 12 times that of $ClNO_2$ measured in the early morning and ~68% higher than the maximum estimated concentration calculated from $ClNO_2$ photolysis in London (Bannan et al. 2015). The maximum Cl concentration produced from Cl_2 and $ClNO_2$ photolysis on the 5th reached 22.5 ×10^3 Cl radicals cm^3 which is approximately 26% of the 85.0 × 10^3 Cl radicals cm^3 maximum calculated value from the photolysis of these two species in Houston in summer (Faxon et al. 2015). This is dominated by the contribution of Cl_2, indicating Cl_2 can be a much more significant source of Cl than $ClNO_2$. On this high flux day, when hourly mean Cl_2 concentrations range between 0 – 7 ppt, the source term is calculated to be between 4 - 21 ppt Cl_2 hr^{-1}, which is slightly lower although consistent with previous studies (Spicer et al. 1998; Finley & Saltzman 2006; Faxon et al. 2015).

The 7th Nov has been highlighted as a day with low photolysis rates and high day time $ClNO_2$ concentrations. On this day, $ClNO_2$ is the dominant Cl source (95%) reaching a maximum of 8.3 x 10^3 Cl radicals cm^{-3} at 9:30 which is ~87% of that calculated for London (Bannan et al. 2015). A mean Cl_2 concentration of 0.3 ppt (less than the LOD of 0.5 ppt) on this day is very low as production of Cl_2 at its maximum, calculated as 0.6 ppt hr^{-1}, is also low. This combined with a low maximum J_{Cl2} = 1.13x10^{-4} hr^{-1} means maximum Cl production from Cl_2 photolysis on this day is very low, generating 2.1 x 10^3 Cl radicals cm^{-3} at 10:00 or a quarter of the maximum contributed by $ClNO_2$ on this day, see Fig 7.

$$Cl^-{}_{(aq)} \xrightarrow{J} \tfrac{1}{2}Cl_{2(g)} \xrightarrow{J_{Cl_2}} Cl \quad (8)$$

The dependency of Cl formation on Cl_2 production and loss highlights the sensitivity of this reaction channel to photolysis is demonstrated on these two days. The production of Cl from $ClNO_2$ is relatively speaking, less sensitive to the solar flux as the production of $ClNO_2$ does not rely on photochemistry but chemical composition cf. (6) and (8). This further highlights the role of photolytic mechanisms in the re-activation of particulate chloride to gaseous chlorine radicals.

4.3. Organic vs inorganic contribution to Cl radical production

Summing the concentrations of the ClOVOCs described in the section above and assuming a uniform photolysis rate J_{CH3OCl} as detailed in the above section, we derive the contribution of total measured ClOVOC to the Cl budget and compare it to the contribution from inorganic Cl measured here (Fig 7). On the high flux day, the Cl concentration reaches 6.9 x 10^3 Cl radicals cm^{-3} at midday, which is 20% greater than the contribution by $ClNO_2$ and 60% less than the contribution of Cl_2 for the same day. On the low flux day, the ClOVOC contribution is 1.8 x 10^3 Cl radicals cm^{-3}, which is ~20% of the $ClNO_2$ contribution on that day and ~85% of the Cl_2 contribution. Like Cl_2, the production of most ClOVOC requires a photolytic step to generate concentrations that can then go on to decompose providing the Cl. Here it is suggested that the organic contribution to Cl production is 15% on the low radiant flux day and 24% on the high flux day.

5. Conclusion

A large suite of inorganic and organic, oxygenated, chlorinated compounds has been identified in ambient, urban air during the wintertime in the UK. Of the 7 organic chlorinated compounds (ClOVOCs) identified here only $C_2H_3O_2ClO$ (tentatively assigned as chloroacetic acid) has previously been reported. No aliphatic or polychlorinated species were detected, although the ToF-CIMS with I^- is sensitive towards them e.g. methyl chloride (CH_3Cl) dimethyl chloride (CH_2Cl_2) and chloroform ($CHCl_3$). The sources of ClOVOCs are mostly photochemical with maxima of up to 140 ppt observed at midday, although $C_3H_7O_3Cl$ and $C_4H_7O_2Cl$ concentrations correlate with NO_x accumulating at low wind speeds, indicating they are produced locally, potentially as the thermal breakdown products of higher mass chlorinated species such as polychlorinated dibenzo-*p*-dioxins/dibenzofurans (PCDD/F) from car exhausts or the oxidation products thereof.

Alongside ClOVOCs, daytime concentrations of Cl_2 and $ClNO_2$ are measured reaching maxima of 17 ppt and 506 ppt respectively. $ClNO_2$ is a source of Cl throughout every day time period measured. Cl_2 shows strong evidence of a daytime production pathway limited by photolysis as well as emission sources evident during the evening and night time.

On a day of high radiant flux (84±14% of idealised values), Cl_2 is the dominant source of Cl, generating a steady state concentration of $16.8x10^3$ Cl radicals cm^{-3} or 57% of the total Cl produced by the photolysis of Cl_2, $ClNO_2$ and ClOVOC with the latter two contributing 19% and 24% respectively. This contrasts with a share of 17% for Cl_2, 68% for $ClNO_2$ and 15% for ClOVOCs on a low radiant flux day (21±14% of idealised values). On the low radiance day not only is the photolysis of all Cl species inhibited, reducing Cl concentrations, but also the formation of Cl_2 and some ClOVOCs by photochemical mechanisms is inhibited thus the variability in contribution between days is highly sensitive to the incidence of sunlight. This further highlights the importance of photochemistry in the re-activation of particulate chloride to gaseous chlorine radicals. Similarly to Cl_2, ClOVOCs can be an important source of Cl although the behaviour of their contribution is similar to Cl_2 relying on high rates of photolysis, rather than high concentrations as is the case for $ClNO_2$.

The contribution of the ClOVOCs to the Cl budget would be better determined if more specific photolysis rates for each compound were available and so would further improve the accuracy of the contribution they make to the Cl budget. In addition, future work should aim to identify the processes leading to the formation of these compounds to better constrain the Cl budget in the urban atmosphere. Further ambient measurements of a broader suite of chlorinated species, as shown here, in different chemical environments would help to better constrain the contribution that chlorine-initiated chemistry has on a global scale.

References

Atkinson, R. et al., 2007. Evaluated kinetic and photochemical data for atmospheric chemistry: Volume III -- gas phase reactions of inorganic halogens. *Atmospheric Chemistry and Physics*, 7, pp.981–1191.

Atkinson, R. et al., 2006. Summary of Evaluated Kinetic and Photochemical Data for Atmospheric Chemistry, Web Version, February 2006. *IUPAC Subcommittee on Gas Kinetic Data Evaluation for Atmospheric Chemistry*, pp.1–60.

Bannan, T.J. et al., 2017. Ground and Airborne U.K. Measurements of Nitryl Chloride: An Investigation of the Role of Cl Atom Oxidation at Weybourne Atmospheric Observatory. *Journal of Geophysical Research: Atmospheres*, 122(20), p.11,154-11,165.

Bannan, T.J. et al., 2015. The first UK measurements of nitryl chloride using a chemical ionization mass spectrometer in central London in the summer of 2012, and an investigation of the role of Cl atom oxidation. *Journal of Geophysical Research*, 120(11), pp.5638–5657.

Borduas, N. et al., 2015. Experimental and theoretical understanding of the gas phase oxidation of atmospheric amides with OH radicals: Kinetics, products, and mechanisms. *Journal of Physical Chemistry A*, 119(19), pp.4298–4308.

Boucher, O. et al., 2009. The indirect global warming potential and global temperature change potential due to methane oxidation. *Environmental Research Letters*, 4(4), p.44007.

le Breton, M. et al., 2012. Airborne observations of formic acid using a chemical ionization mass spectrometer. *Atmospheric Measurement Techniques*, 5(12), pp.3029–3039.

le Breton, M. et al., 2018. Chlorine oxidation of VOCs at a semi-rural site in Beijing: Significant chlorine liberation from ClNO2 and subsequent gas and particle phase Cl-VOC production. *Atmospheric Chemistry and Physics Discussions*, (January), pp.1–25.

le Breton, M. et al., 2017. Enhanced ozone loss by active inorganic bromine chemistry in the tropical troposphere. *Atmospheric Environment*, 155, pp.21–28.

le Breton, M. et al., 2014. Simultaneous airborne nitric acid and formic acid measurements using a chemical ionization mass spectrometer around the UK: Analysis of primary and secondary production pathways. *Atmospheric Environment*, 83(3), pp.166–175.

le Breton, M. et al., 2014. The first airborne comparison of N2O5 measurements over the UK using a CIMS and BBCEAS during the RONOCO campaign. *Anal. Methods*, 6(24), pp.9731–9743.

Butler, J., 2000. Better budgets for methyl halides? *Nature*, 403(6767), pp.260–1.

Carlton, A.G. et al., 2006. Link between isoprene and secondary organic aerosol (SOA): Pyruvic acid oxidation yields low volatility organic acids in clouds. *Geophysical Research Letters*, 33(6), pp.2–5.

Crowley, N. et al., 1994. CH3OCI: UV/visible absorption cross sections, J values and atmospheric significance. *Journal of Geophysical Research*, 99(D10), p.20,683-20,688.

Deiber, G. et al., 2004. Uptake study of ClONO2 and BrONO2 by Halide containing droplets. *Atmospheric Chemistry and Physics*, 4(5), pp.1291–1299.

Eigen, M. & Kustin, K., 1962. The Kinetics of Halogen Hydrolysis. *Journal of the American Chemical Society*, 84(8), pp.1355–1361.

Faxon, C., Bean, J. & Ruiz, L., 2015. Inland Concentrations of Cl2 and ClNO2 in Southeast Texas Suggest Chlorine Chemistry Significantly Contributes to Atmospheric Reactivity. *Atmosphere*, 6(10), pp.1487–1506.

Finley, B.D. & Saltzman, E.S., 2006. Measurement of Cl2 in coastal urban air. *Geophysical Research Letters*, 33(11), pp.6–9.

Foster, K.L. et al., 1999. Techniques for quantifying gaseous HOCl using atmospheric pressure ionization mass spectrometry. *Physical Chemistry Chemical Physics*, 1(24), pp.5615–5621.

Fuentes, M.J. et al., 2007. Pyrolysis and combustion of waste lubricant oil from diesel cars: Decomposition and pollutants. *Journal of Analytical and Applied Pyrolysis*, 79(1–2 SPEC. ISS.), pp.215–226.

Ghernaout, D. & Ghernaout, B., 2010. From chemical disinfection to electrodisinfection: The obligatory itinerary? *Desalination and Water Treatment*, 16(1–3), pp.156–175.

Heal, M. et al., 1995. On the Development and Validation of FAGE for Local Measurement of Tropospheric OH and HO2. *Journal of the Atmospheric Sciences*, 52(19), pp.3428–3441.

Heeb, N. V. et al., 2013. PCDD/F formation in an iron/potassium-catalyzed diesel particle filter. *Environmental Science and Technology*, 47(12), pp.6510–6517.

Hoffman, R.C. et al., 2003. Knudsen cell studies of the reactions of N2O5 and ClONO2 with NaCl: development and application of a model for estimating available surface areas and corrected uptake coefficients. *Physical Chemistry Chemical Physics*, 5(9), pp.1780–1789.

Hossaini, R. et al., 2016. A global model of tropospheric chlorine chemistry: Organic versus inorganic sources and impact on methane oxidation. *Journal of Geophysical Research: Atmospheres*, 121(23), p.14,271-14,297.avai

Huang, B. et al., 2014. Chlorinated volatile organic compounds (Cl-VOCs) in environment - sources, potential human health impacts, and current remediation technologies. *Environment International*, 71, pp.118–138.

Keene, W.C. et al., 1993. Measurement Technique for Inorganic Chlorine Gases in the Marine Boundary Layer. *Environmental Science and Technology*, 27(5), pp.866–874.

Kercher, J.P., Riedel, T.P. & Thornton, J.A., 2009. Chlorine activation by N2O5: simultaneous, in situ detection of ClNO2 and N2O5 by chemical ionization mass spectrometry. *Atmos. Meas. Tech.*, 2(1), pp.193–204.

Lawler, M.J. et al., 2011. HOCl and Cl2 observations in marine air. *Atmospheric Chemistry and Physics*, 11(15), pp.7617–7628.

Leather, K.E. et al., 2012. Temperature and pressure dependence of the rate coefficient for the reaction between ClO and CH3O2 in the gas-phase. *Physical Chemistry Chemical Physics*, 14, pp.3425–3434.

Lee, B.H. et al., 2014. An Iodide-Adduct High-Resolution Time-of-Flight Chemical-Ionization Mass Spectrometer: Application to Atmospheric Inorganic and Organic Compounds. *Environmental Science & Technology*, 48(11), pp.6309–6317.

Leu, M.-T. et al., 1995. Heterogeneous Reactions of HNO3(g) + NaCl(s) .fwdarw. HCl(g) + NaNO3(s) and N2O5(g) + NaCl(s) .fwdarw. ClNO2(g) + NaNO3(s). *The Journal of Physical Chemistry*, 99(35), pp.13203–13212.

Liao, J. et al., 2014. High levels of molecular chlorine in the Arctic atmosphere. *Nature Geoscience*, 7(2), pp.91–94.

Liu, X. et al., 2017. High levels of daytime molecular chlorine and nitryl chloride at a rural site on the North China Plain. *Environmental Science & Technology*, (2), p.acs.est.7b03039.

Ma, Y. et al., 2013. Rapid modification of cloud-nucleating ability of aerosols by biogenic emissions. *Geophysical Research Letters*, 40(23), pp.6293–6297.

Mandronich, S., 1987. Photodissociation in the Atmosphere Actinic Flux and the Effects of Ground Reflections and Clouds. *Journal of Geophysical Research*, 92, pp.9740–9752.

Mielke, L.H. et al., 2013. Heterogeneous formation of nitryl chloride and its role as a nocturnal NOx reservoir species during CalNex-LA 2010. *Journal of Geophysical Research Atmospheres*, 118(18), pp.10638–10652.

Mielke, L.H. et al., 2016. Ubiquity of ClNO2 in the urban boundary layer of Calgary, Alberta, Canada. *Canadian Journal of Chemistry*, 94(4), pp.414–423.

Mielke, L.H., Furgeson, A. & Osthoff, H.D., 2011. Observation of ClNO2 in a mid-continental urban environment. *Environmental science & technology*, 45, pp.8889–96.

Nguyen, T.B. et al., 2015. Rapid deposition of oxidized biogenic compounds to a temperate forest. *Proceedings of the National Academy of Sciences*, 112(5), pp.E392–E401.

Osthoff, H.D. et al., 2008. High levels of nitryl chloride in the polluted subtropical marine boundary layer. *Nature Geoscience*, 1(5), pp.324–328.

Oum, K.W., 1998. Formation of Molecular Chlorine from the Photolysis of Ozone and Aqueous Sea-Salt Particles. *Science*, 279(5347), pp.74–76.

Priestley, M. et al., 2018. Observations of isocyanate, amide, nitrate and nitro compounds from an anthropogenic biomass burning event using a TOF-CIMS. *Journal of Geophysical Research*, Accepted: 2018-02-24, DOI: 10.1002/2017JD027316.

Phillips, G.J. et al., 2012. Significant concentrations of nitryl chloride observed in rural continental Europe associated with the influence of sea salt chloride and anthropogenic emissions. *Geophysical Research Letters*, 39(10), pp.1–5.

Reed, C. et al., 2016. Interferences in photolytic NO2 measurements: Explanation for an apparent missing oxidant? *Atmospheric Chemistry and Physics*, 16(7), pp.4707–4724.

Reyes-Villegas, E. et al., 2017. Simultaneous Aerosol Mass Spectrometry and Chemical Ionisation Mass Spectrometry measurements during a biomass burning event in the UK: Insights into nitrate chemistry. *Atmospheric Chemistry and Physics Discussions*, (July), pp.1–22.

Riedel, T.P. et al., 2012. Nitryl chloride and molecular chlorine in the coastal marine boundary layer. *Environmental Science and Technology*, 46(19), pp.10463–10470.

Roberts, J.M. et al., 2008. N2O5 oxidizes chloride to Cl2 in acidic atmospheric aerosol. *Science*, 321(5892), p.1059.

Sarwar, G. et al., 2014. Importance of tropospheric ClNO2 chemistry across the Northern Hemisphere. *Geophysical Research Letters*, 41(11), pp.4050–4058.

Simon, M. et al., 2016. Detection of dimethylamine in the low pptv range using nitrate chemical ionization atmospheric pressure interface time-of-flight (CI-APi-TOF) mass spectrometry. *Atmospheric Measurement Techniques*, 9(5), pp.2135–2145.

Sipilä, M. et al., 2015. Bisulfate - Cluster based atmospheric pressure chemical ionization mass spectrometer for high-sensitivity (< 100 ppqV) detection of atmospheric dimethyl amine: Proof-of-concept and first ambient data from boreal forest. *Atmospheric Measurement Techniques*, 8(10), pp.4001–4011.

Slaper, H. et al., 1995. Comparing ground-level spectrally resolved solar UV measurements using various instruments: A technique resolving effects of wavelength shift and slit width. *Geophysical Research Letterse*, 22(20), pp.2721–2724.

Smedley, A.R.D. et al., 2012. Total ozone and surface UV trends in the United Kingdom: 1979-2008. *International Journal of Climatology*, 32(3), pp.338–346.

Spicer, C.W. et al., 1998. Unexpectedly high concentrations of molecular chlorine in coastal air. *Nature*, 394(June 1996), pp.353–356.

Thornton, J.A. et al., 2010. A large atomic chlorine source inferred from mid-continental reactive nitrogen chemistry. *Nature*, 464(7286), pp.271–274.

Vogt, R., Crutzen, P.J. & Sander, R., 1996. A mechanism for halogen release from sea-salt aerosol in the remote marine boundary layer. *Nature*, 383(6598), pp.327–330.

Wang, D.S. & Ruiz, L.H., 2017. Secondary organic aerosol from chlorine-initiated oxidation of isoprene. , (May), pp.1–25.

Wang, W.H. & Finlayson-Pitts, B.J., 2001. Unique markers of chlorine atom chemistry in coastal urban areas: The reaction with 1,3-butadiene in air at room temperature. *Journal of Geophysical Research-Atmospheres*, 106(D5), pp.4939–4958.

Wang, X. et al., 2017. Observations of N2O5 and ClNO2 at a polluted urban surface site in North China: High N2O5 uptake coefficients and low ClNO2 product yields. *Atmospheric Environment*, 156(3), pp.125–134.

Wong, J.P.S. et al., 2017. Observations and impacts of bleach washing on indoor chlorine chemistry. *Indoor Air*, 27(6), pp.1082–1090.

Yokouchi, Y. et al., 2000. A strong source of methyl chloride to the atmosphere from tropical coastal land. *Nature*, 403, pp.295–298.

Atmos. Chem. Phys. Discuss., https://doi.org/10.5194/acp-2018-236
Manuscript under review for journal Atmos. Chem. Phys.
Discussion started: 7 March 2018

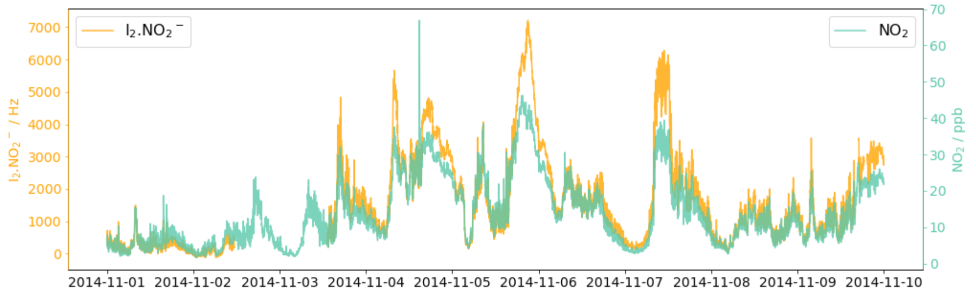

Fig 1. NO_2 measured at the whitworth observatory overlayed with $I_2.NO_2^-$ measured on the ToF-CIMS. NO_2 is overestimated by the ToF-CIMS at high concentrations. This is potentially due to the degredation of NOy species in the IMR.

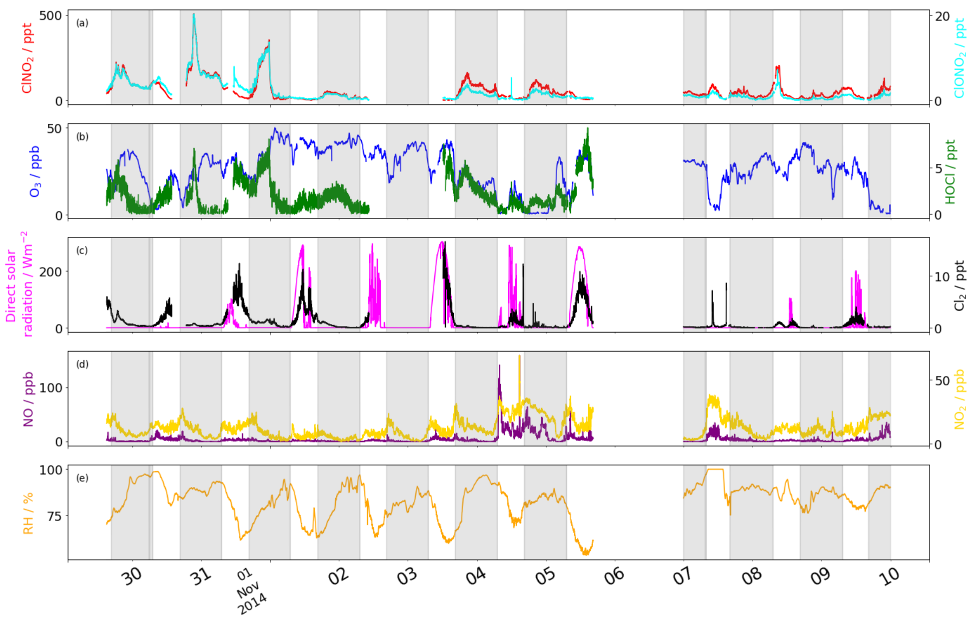

Fig 2. Time series of a. $ClNO_2$ (ppt) and $ClONO_2$ (ppt). b. HOCl (ppt) and O_3 (ppb). c. Cl_2 (ppt) and direct solar radiation (Wm^{-2}). d. NO (ppb) and NO_2 (ppb). e. Relative humidity (%). Data is removed during bonfire night (5^{th}-6^{th}) and HOCl data is discounted thereafter due to a persistent interference which was not present earlier.

Atmos. Chem. Phys. Discuss., https://doi.org/10.5194/acp-2018-236
Manuscript under review for journal Atmos. Chem. Phys.
Discussion started: 7 March 2018

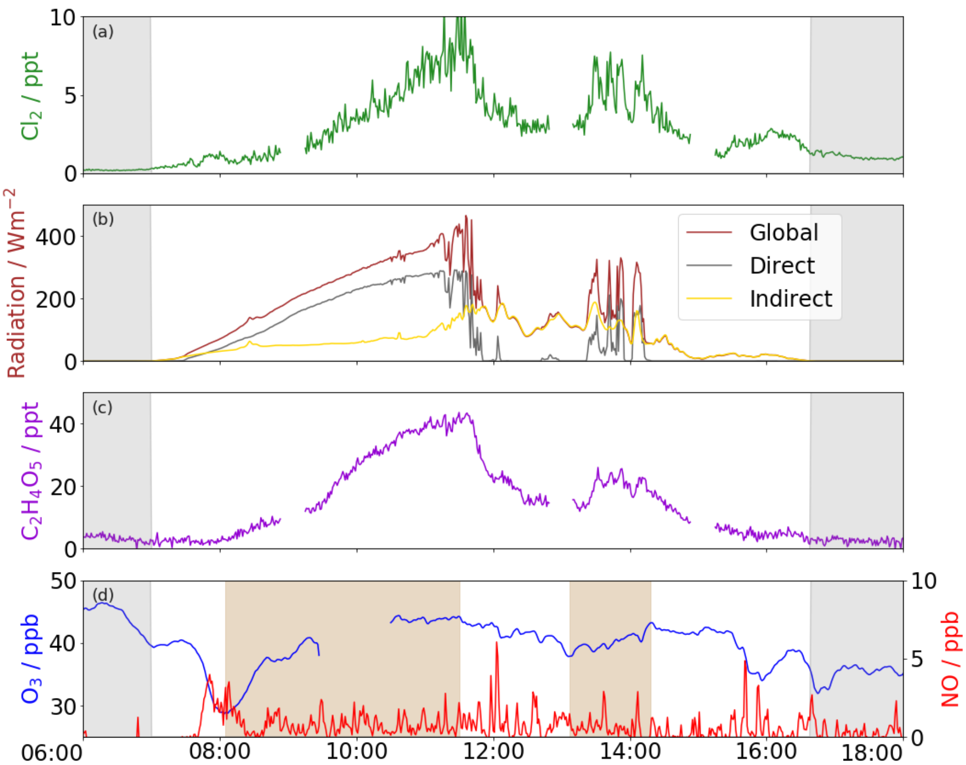

Fig 3. Time series for the day of 1st Nov 2014. a. Cl_2 b. solar radiation (global, direct and indirect) c. photochemical marker $C_2H_4O_5$ d. O_3 and NO_x where highlighted boxes demonstrate $\frac{\Delta[O_3]}{\Delta t}$ is increasing. The increase in concentration of Cl_2, $C_2H_4O_5$ and O_3 production when VOC limited are strongly coupled
600 **to direct solar radiation. Greyed areas are night time.**

Atmos. Chem. Phys. Discuss., https://doi.org/10.5194/acp-2018-236
Manuscript under review for journal Atmos. Chem. Phys.
Discussion started: 7 March 2018

Atmospheric Chemistry and Physics Discussions

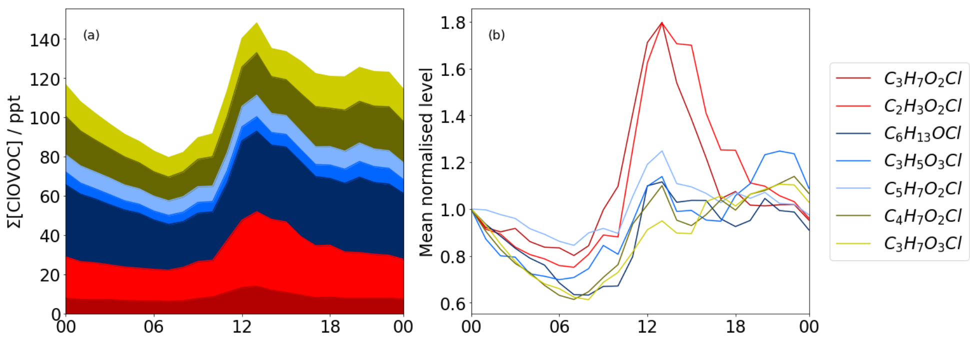

Fig 4. Diurnal profiles of Cl VOCs. a. Stacked plot showing total Cl VOC concentration. b. The first data
605 **point of each diurnal trace is mean normalised to 1.0. Reds show photochemical dominated signals with maxima at midday whereas yellow and blue traces show a more typical diurnal concentration profile associated with changes in boundary layer height indicating these species have longer lifetimes.**

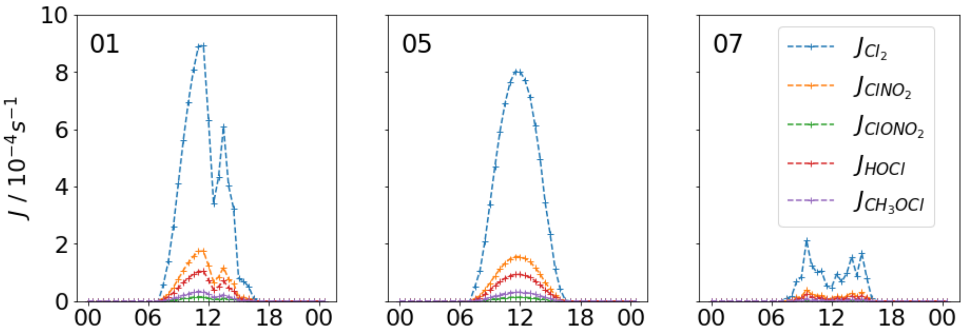

610 **Fig 5. Transmission scaled J values for Cl_2, $ClNO_2$ $ClNO_3$ and HOCl for the 1st, 5th and 7th of Nov. The 1st had high photolysis rates in the morning that were reduced during the afternoon. The 5th is the closest to a full day's ideal photolysis. The 7th shows very weak photolysis.**

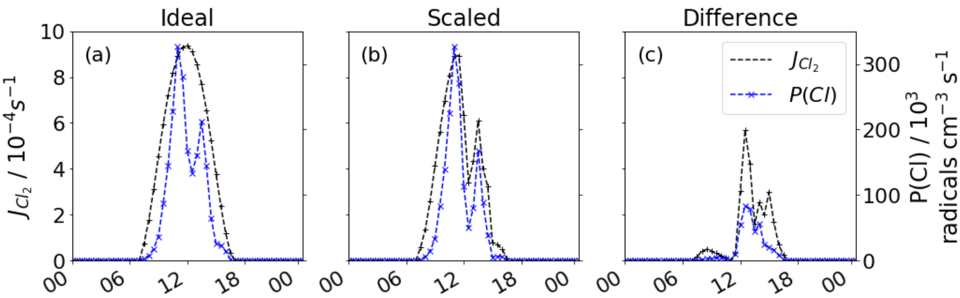

615

Fig 6. Diurnal profile for 1st Nov of: a. idealised J_{Cl2} and P(Cl), b. scaled J_{Cl2} and P(Cl), c. the difference between a and b. Transmission efficiency scaled photolysis reduce P(Cl) from Cl_2 photolysis.

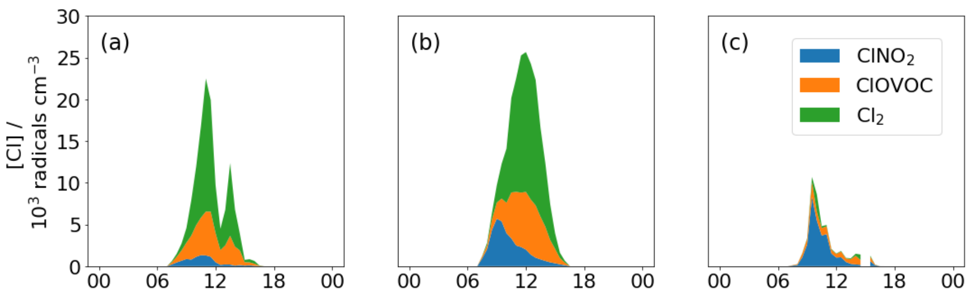

620 **Fig 7. Steady state concentration of Cl from $ClNO_2$, Cl_2 and total ClOVOC photolysis for a. 1st Nov, b. 5th Nov, and c. 7th Nov. The importance of $ClNO_2$ during the morning is most evident on the 5th with a diminishing contribution throughout the day. On the high flux days, Cl_2 and ClOVOCs are the most important source of Cl but on the low flux day $ClNO_2$ is most important.**